



Research Article

Investigation of Controlled Release Molecular Mechanism of Oil Phase in Spilanthol Emulsion: Development and *In Vitro*, *In Vivo* Characterization

Degong Yang,¹ Wanlin Li,² Liang Fang,¹ and Chao Liu^{1,3}

Received 5 April 2019; accepted 12 June 2019; published online 20 June 2019

Abstract. The aim of the present study was to develop a spilanthol emulsion and investigate the effect of oil and drug physicochemical properties on drug release and skin retention at molecular level. Formulation factors including oil, emulsifier, and humectant were investigated by *in vitro* skin retention/permeation study and the optimized formulation was evaluated *in vitro* and *in vivo*. In addition, the controlled release effect of oil was characterized using drug emulsion distribution study, drug release study, FT-IR, and molecular modeling. The optimized emulsion (squalane as oil phase) obtained the maximum skin retention ($118.71 \pm 10.30 \mu\text{g/g}$), which significantly restored skin hydroxyproline content ($23.99 \pm 2.21 \mu\text{g/g}$), compared with the positive group ($14.75 \pm 1.84 \mu\text{g/g}$) and the negative group ($15.55 \pm 2.03 \mu\text{g/g}$). It was caused by high drug release of squalene and good drug–skin miscibility. FT-IR and molecular modeling showed that spilanthol (SPI) interacted with squalene through Van der Waals force, which was weaker than a hydrogen bond formed with other oils, thus exhibited good drug release properties. And the released drug was stored in the skin due to good drug–skin miscibility, which was proved by miscibility calculation and molecular modeling. In conclusion, an effective emulsion was developed and the controlled release effect of oil phase was proved through drug–excipient interaction.

KEY WORDS: emulsion; drug release; molecular interaction; miscibility; skin retention.

INTRODUCTION

Spilanthol (SPI) is a prominent representative of the N-alkylamides, which can be found in several plants (1). In addition, it has various biological activities, mainly including anti-wrinkle, analgesic, antioxidant, antimalarial, and antifungal (2,3). More importantly, it was reported as an active ingredient with the effect of relaxing muscle and smoothing skin (4). SPI reduced dramatically crow's feet and inhibited evident contractions in subcutaneous muscles of the face skin (5). The structure of SPI is illustrated in Fig. 1 and the physicochemical properties of SPI are suitable for transdermal drug delivery system (TDDS), such as its molecular weight which is 221.3 Da, $\log P$ is 3.2, and melting point is 23°C (6). Therefore, it is designed as emulsion to achieve topical efficacy, which is suitable for administration as anti-wrinkle preparation.

SPI was prepared through gel and emulsion according to previous reports (7,8), but no further study was conducted.

Moreover, in the last several decades, the preparation and clinical efficacy have dominated the main space in the development of emulsion (9–11). However, the formulation screening was a complicated process due to the complex components of emulsion, which were mainly classified into oil phase, aqueous phase, and emulsifier. The effect of oil was considered extremely important, but little research was conducted to illustrate the role of oil on the transdermal drug delivery process at a molecular level. Generally, drug release was an important step for the whole TDDS. The factors that influence drug release from emulsion were the droplet size, morphology, and viscosity of the emulsions according to the previous literatures (12,13). Generally, emulsion itself is a controlled release system, that drug is entrapped in the internal phase then diffuse through the external phase to the skin surface and slowly gets absorbed. Internal phases act as a reservoir of drug (14). In the drug delivery process, drug–matrix interaction is considered one of the most important factors that influence the drug release process, and stratum corneum of the skin was the main barrier for the drug absorption into skin and systemic circulation (15). Although emulsion contains low proportion of oil, the effect of oil on drug release is not able to be ignored. Moreover, molecule interaction between drug and excipient plays the crucial role in the drug delivery process and gains widespread concern (16,17). In conclusion, there

¹Department of Pharmaceutical Sciences, Shenyang Pharmaceutical University, 103 Wenhua Road, Shenyang, 110016, Liaoning, China.

²Department of Basic Medical Sciences, Shenyang Medical College, 146 Huanghe North Street, Shenyang, 110034, Liaoning, China.

³To whom correspondence should be addressed. (e-mail: liuchao1185@gmail.com)

are two main issues to be solved, drug–skin miscibility and effect of molecular interaction on drug release behavior.

The objective of the present work was to develop spilanthol emulsion and investigate the effect of oil and drug physicochemical properties on drug release and skin retention at the molecular level. The formula of emulsion was screened using *in vitro* skin permeation and retention study, especially the effect of oils, including squalene, lipex shea light (LIPEX), isononyl isononanoate (ININ), and dipalmitoyl phosphatidylglycerole (DPPG), and their structures were showed in Fig. 1. The optimized emulsion was evaluated using *in vivo* tissue distribution study, pharmacodynamic study and safety study using animal model. Drug–skin miscibility was characterized by the miscibility calculation and molecular modeling to illustrate drug–skin retention pattern. The effect of oil on the drug release process was illustrated using physical property characterization, drug emulsion distribution study, and drug release study. Finally, the drug–oil molecular interaction was characterized using FT-IR and molecular modeling to illustrate the effect of oil on drug release at the molecular level.

MATERIALS AND METHODS

Materials and Animals

Spilanthol was purchased from Nanjing Zelang Medical Technology Co., Ltd. (Jiangsu, China). The LIPEX, ININ, DPPG, squalene, Delta, Simulsol 165, hyaluronic acid, glycerinum, trehalose, and 1,3-butanediol were purchased from Puen Biochemical Technology Co., Ltd. (Shanghai, China). Poloxamer 188 (F68) was provided from BASF China Co., Ltd. (Shanghai, China). MONTANOV 68 was provided from Seppic (Paris, France). All other chemicals and solvent were reagent grade and obtained commercially.

Wistar rats (male, No.:211002300016752) weighing 180–220 g and Japanese white rabbits (male, No.:211002600000572) weighing 1.5–2.5 kg were supplied by the Experimental Animal Center of Shenyang

Pharmaceutical University (Shenyang, China). Kunming mice (male, No.:211,002,300,018,602) weighing 18–22 g was supplied by the Experimental Animal Center of Academy of Military Medical Sciences (Beijing, China). All the procedures were performed in accordance with the NIH Guidelines for the Care and Use of Laboratory Animals and were approved by the Animal Ethics Committee of Shenyang Pharmaceutical University.

Preparation of Emulsion

The emulsion was prepared using mechanical dispersion method. LIPEX as oil phase, Simulsol 165 as emulsifier, and water as aqueous phase were mixed and prepared into basic emulsion as control. Emulsifier (weight fraction 5%) and oil (weight fraction 10%) were accurately weighed and mixed. The obtained oil phase was heated to 70°C and mixed to obtain a homogeneous solution. Afterwards, SPI (drug loading of 1%) and humectant (weight fraction of 5%) were accurately weighed and mixed. Then, proper amount of water was added and heated to 70°C. Then, oil phase and water phase were mixed and dispersed using high-speed homogenizer (FJ-200S) at 4000 r/min for 10 min.

In Vitro Drug–Skin Permeation/Retention Study

The *in vitro* drug–skin permeation study was performed with a vertical diffusion cell in a multi-functional transdermal diffusion instrument at 32°C (18). The emulsion was applied as the donor phase, and PBS + 20% PEG400 (4 mL) was used as the receptor fluid to ensure sink condition. Receptor fluid (2.0 mL) was withdrawn for analysis in 8 h at a determined time point. Sample was analyzed with Hitachi HPLC system (pump L-2130, UV detector L-2420, autosampler L-2200, T-2000L workstation) and Diamonsil ODS (5 μ m, 200 \times 4.6 mm). The mobile phase was methanol: water = 76:24 (v/v) with a flow rate of 1 mL/min. The column temperature was kept at 40°C and the detection wavelength was 237 nm.

The *in vitro* drug–skin retention study was performed according to the previous literature (19). At the end of the drug–skin permeation study, the skin was taken from the cell to collect the retention drug as follows: the residual emulsion on the skin was wiped off by cotton swab with ethanol and then moisture on the skin surface was wiped. The diffusion field of skin was cut, immersed into methanol, and sonicated for 20 min, followed by centrifugation for 5 min at 16,000 rpm. The supernatant was collected for HPLC analysis.

Drug–Skin Miscibility Calculation

Drug–skin miscibility calculation was carried out to illustrate drug–skin retention behavior. And solubility parameters (δ) of drug and ceramide-NS, instead of skin, were calculated using group contribution method. Fedors' method (20) was chosen due to the parameters of large number of different groups provided. Solubility parameters were obtained as follows:

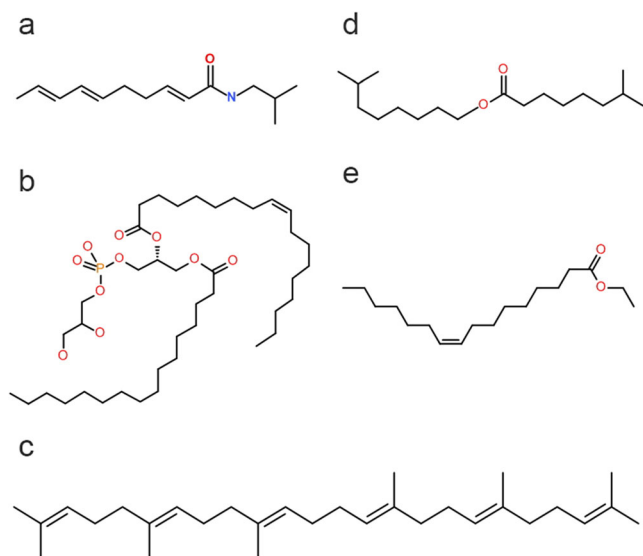


Fig. 1. Chemical structures of **a** SPI, **b** DPPG, **c** squalene, **d** ININ, and **e** LIPEX

$$\delta = \sqrt{\frac{\sum_i(\Delta E)_i}{\sum_i(\Delta V)_i}} \quad (1)$$

where δ ((cal/cm³)^{0.5}) was the solubility parameter, $\sum_i(\Delta E)_i$ (cal/mol) was the sum of cohesive, and $\sum_i(\Delta V)_i$ was the sum of molar volumes (cm³/mol).

Drug-PSA miscibility was predicted using the Flory equation based on solubility parameters δ , which was expressed in the following equation (21):

$$\Phi = \exp-[1 + X_1] = \exp-\left[1.34 + \frac{V_1}{RT} \times (\delta_1 - \delta_2)^2\right] \quad (2)$$

where Φ was the volume fraction of solute, drug volume \approx drug mass fraction. V_1 was the molar volume of the drug ($V_{SPI} = 246.8$ cm³/mol), δ_1 was the solubility parameter of the drug, δ_2 was the solubility parameter of the skin, R was the gas constant (8.314 J × K⁻¹ mol⁻¹), and T was the selected temperature (25°C (298 K)). Thus, the parameter of Φ was used to predict the solubility of SPI in skin. High drug fraction in the skin indicated good drug-skin miscibility.

Drug Emulsion Distribution Study

Drug emulsion distribution study was performed by a shake-flask method. Water and oils including squalene, LIPEX, ININ, and DPPG were weighed accurately at the weight ratio of 5:1, which was consistent with the formulation composition fraction. Then, the sample was shaken for 24 h at 32°C and separated by centrifugation. Finally, drug content in both water and oil layer were analyzed by HPLC.

In Vitro Drug Release Study

In vitro drug release study was carried out to investigate the effect of oil on drug release from emulsion. The experiment was performed with a vertical diffusion cell in a multi-functional transdermal diffusion instrument at 32°C. The emulsion was added on the Cellophane® membrane, and a mixture of PBS and 20% PEG400 was used as the receptor fluid. The receptor fluid (2.0 mL) is sampled at the time points 2, 4, 6, and 8 h, and equal volume of fresh medium was added. The samples were collected for HPLC analysis.

Apparent Viscosity Determination

The apparent viscosity of emulsion containing different oils was measured using the SNB-1 digital rotary viscometer (Shanghai, China). The emulsion was determined with 10 rpm using the NO. 27 rotor at 25°C. All determinations were in triplicate.

Droplet Size Characterization

The droplet size of the emulsion containing different oils was determined using particle size analyzer (Zetasizer Nano ZS 90, Malvern, Worcestershire, UK). Emulsion was diluted with distilled water to obtain appropriate concentration of emulsion. The experiments were in triplicate.

Fourier Transform Infrared Spectroscopy

The FT-IR spectra were obtained with a Bruker Vertex 70 spectrometer (Billerica, USA) to investigate the interaction between drug and oils. Pure drug, pure oil, and mixture were dissolved in ethyl acetate and dropwise added onto the KBr pellet and then dried at 50°C for 5 min. The spectra were obtained through 128 scans over the spectral range of 4000–400 cm⁻¹. Spectra data was obtained using OPUS software (Bruker Optics, Billerica, USA).

Molecular Modeling

Molecular modeling study was utilized to provide direct molecular details of drug-oil interaction and drug-skin miscibility, using the software package Materials Studio (version 7.0, Accelrys Inc., San Diego, CA, USA). Initially, all compound models were built and subjected to geometry optimization employing the Forcite module using the COMPASSII force field (22). Moreover, blend module was used to calculate the energy of mixing (23). The modeling of miscibility between drug and skin, drug and water were also conducted. Ceramide (CerNS) was used as a skin molecular model (24). Forcite module was used to calculate the energy of system and the miscibility between them.

In Vivo Drug Tissue Distribution Study

In vivo drug tissue distribution study was conducted using male Kunming mice (20 g ± 2 g). The mice's abdominal hair was removed 24 h in advance. According to predetermined time points 1, 2, 4, 6, 8, 12, and 24 h, mice were assigned randomly into seven groups ($n = 4$) according to time points. Emulsion (100 mg) was applied to the skin (45 mg/kg). At a predetermined time point, blood sample (0.5 mL) was collected into a vacuum propylene tube, and skin and muscle were removed after execution of mice.

Plasma sample extraction process was summarized as follows: internal standard (20 μL, 200 μg/mL, cnidium lactone/methanol solution) and methanol (280 μL) were added into the plasma sample (1000 μL), and then mixture was vortexed for 1 min. After that, the mixture was separated by centrifugation at 16,000 rpm for 10 min, and the supernatant was collected for HPLC analysis. The skin and muscle samples were extracted as follows: the tissue sample was taken and weighed. Internal standard (20 μL) and methanol (380 μL) were added into the sample, and then sonicated for 20 min. The extract was separated by centrifugation at 16,000 rpm for 10 min and the supernatant was collected.

The Pharmacodynamic Evaluation

The In Vivo Anti-aging Effect Evaluation

Male Wistar rats (200 ± 10 g) were used for pharmacodynamic evaluation. The back hair was removed using an electric clipper. The animals were maintained in a temperature and humidity controlled environment with 12:12 h light-dark cycle. Feed and water were available freely.

Rats were randomly divided into four groups ($n = 6$): control group (without UVB exposure), positive control group (with UVB exposure), negative control group (with UVB exposure and blank matrix), and administration group (with UVB exposure and emulsion). The rats were exposed to UVB radiation (400 mJ/cm^2) for five times per week lasting 4 weeks (25). Blank matrix and emulsion were respectively applied to the back ($5 \text{ cm} \times 5 \text{ cm}$) of rats every 24 h. After the experiment, skin samples were collected and photographed after execution for further experiments.

Skin Hydroxyproline Determination

Hydroxyproline content in the skin indicated collagen content; thus, it was determined as an indicator of skin aging degree quantitatively (26). Rat skin was accurately weighed and homogenized with physiological saline in ice water bath. The content of the hydroxyproline (C) was calculated as follows:

$$C = 5 \times \frac{OD_{\text{sample}} - OD_{\text{blank}}}{OD_{\text{standard}} - OD_{\text{blank}}} \times \frac{V_{\text{medium}}}{m_{\text{sample}}} \quad (3)$$

Redistilled water (0.25 mL) and digestive juice (0.05 mL) was set as the blank group, and standard solution (0.25 mL) and prepared digestive juice (0.05 mL) was set as the standard group. Then, 0.5 mL prepared reagent (I), 0.5 mL reagent (II), and 1.0 mL reagent (III) were added. The mixture was separated by centrifugation at 3500 rpm for 10 min, and 100 μL supernatant was collected for automatic enzyme marker analysis (Varioskan Flash, Thermo Scientific). The wavelength was 550 nm.

Safety Evaluation

Skin irritation test was conducted using rabbits. The back hair of the rabbit was removed before the experiment ($n = 6$). Administration area was $2.5 \text{ cm} \times 2.5 \text{ cm}$. 10% sodium dodecyl sulfate (0.5 mL) was spread on the skin surface in the positive group. Moreover, the emulsion was applied on the rabbit skin surface and covered with cellophane. The residue preparation was removed after 8 h. The skin reaction area was recorded at the time points 1, 24, 48, and 72 h after the preparation was removed.

Statistical Data Analysis

The experiment data were presented as mean \pm standard deviation (S.D.). Significant difference between groups was applied with the Student t -test or ANOVA. The level for significance was set at $p \leq 0.05$.

RESULTS

The Oil Phase Optimization

The effect of oil on SPI skin retention and permeation was investigated, including LIPEX (as control), squalane, ININ, and DPPG as oil phase. The skin permeation and retention amount of emulsions with four oils were presented in Fig. 2. The drug permeation amount was much lower

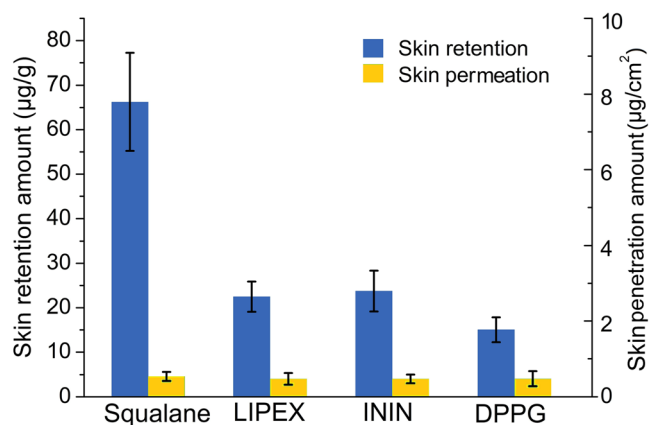


Fig. 2. The cumulative amount and the skin retention amount of SPI with different oils ($n = 4$)

compared with the skin retention amount. The emulsion containing squalane contributed the highest skin retention amount ($65.23 \pm 11.99 \mu\text{g/g}$, $p < 0.05$). Thus, squalane was selected as the oil phase for further studies.

The Emulsifier Optimization

Emulsifier affected the drug–skin retention and the stability of emulsion. The effect of emulsifier was investigated using four emulsifiers with adequate HLB value including Simulsol 165, F68, Delta, and MONTANOV. As shown in Fig. 3, the skin retention amount of emulsion containing Simulsol 165, F68, and Delta was significantly higher than that containing MONTANOV ($p < 0.05$). Moreover, Fig. 4 showed that the emulsions containing Simulsol 165 and F68 were unstable. As a result, Delta was selected as the emulsifier for further studies.

The Humectant Optimization

To further investigate the effect of humectants, four different humectants (HA, trehalose, glycerin, 1,3-butanediol) were tested in the *in vivo* skin permeation study. As presented in Fig. 5, the skin retention amount of HA was highest ($118.71 \pm 10.30 \mu\text{g/g}$), thereby HA was selected as the humectant for further studies.

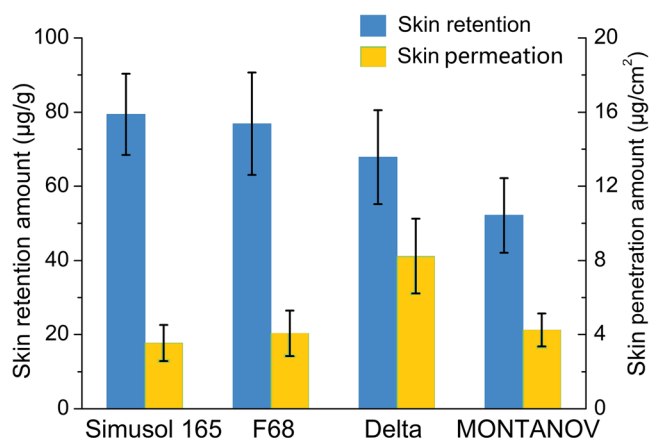


Fig. 3. The cumulative amount and the skin retention amount of SPI with different emulsifiers ($n = 4$)



Fig. 4. The stability of emulsion with different emulsifiers

Drug–Skin Miscibility Study

Drug–Skin Miscibility Calculation

Drug–skin miscibility was an important problem, which determined that drug mainly was accumulated in the skin or penetrated skin into blood, particularly with the increased use of transdermal and topical drug delivery systems. The solubility parameters of drug and CerNS were calculated as 17.85 and 18.89, respectively. According to Eq. (2), drug fraction in skin was predicted, $\Phi = 89\%$, which indicated that there is a good miscibility between drug and skin. The miscibility between drug and water was not good enough, only about 5.3×10^{-5} g/g according to the results in Table 1.

Molecular Modeling

It came into conclusion in previous study that lower system total energy resulted in better miscibility (27). Molecular modeling results showed that the total energy of SPI–SPI system was -84.49 kcal/mol. When CerNS and water were added, total energy of SPI–CerNS and SPI–H₂O systems were -175.03 and -41.73 kcal/mol, respectively, which proved that SPI–CerNS system was more stable and indicated SPI was inclined to dissolve in the CerNS, other than water. At the same time, it was inferred that drug possessed a remarkable skin retention ability.

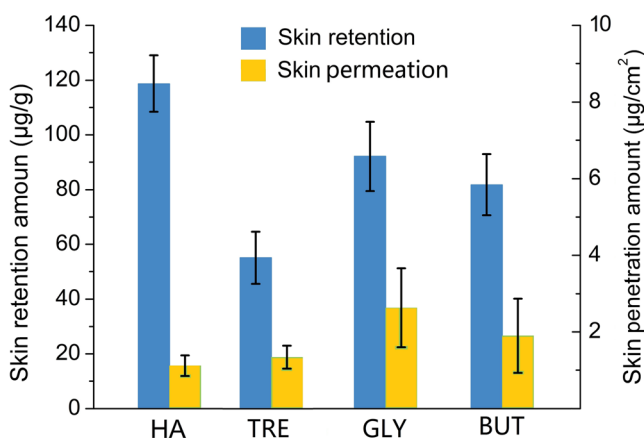


Fig. 5. The cumulative amount and the skin retention amount of spilanthol with different humectants ($n = 4$)

Effect of Oil on Drug Release

Drug Emulsion Distribution Study

The results of drug emulsion distribution study were demonstrated in Table 1. It was proved that drug mainly existed in the oil phase ($C_{oil} \gg C_{water}$). As a result, the oil was the key matrix for emulsion. We proceed with consideration of the role of oil in the emulsion.

In Vitro Drug Release Study

The oil was the main dispersion medium according to drug emulsion distribution study, and the selection of oil was pivotal for drug release behavior. In Fig. 6, the emulsion containing squalane exhibited a significant high drug release amount ($p < 0.05$).

The correlation analysis between drug release amount and skin retention amount was performed and showed in Fig. 7. The above result indicated that there was a good linear relationship between drug release and skin retention, and it indicated that the drug–skin retention was controlled by release behavior. The results indicated that the release behavior of SPI determined the drug retention amount in the skin.

The Apparent Viscosity and Droplet Size of the Emulsion

The results of apparent viscosity and droplet size characterization of the emulsions containing different oils were shown in Table 1. Clearly, there was no significant difference about viscosity and droplet size. As a result, it also provided the basis for studying the molecular mechanism of the oil on the drug release behavior.

FT-IR Study

FT-IR spectroscopy was used to characterize the drug–oil intermolecular interactions. In Fig. 8, The IR band at 3469.62 cm^{-1} for the drug was assigned to NH stretching vibrations. The NH peak wavenumber of drug–squalane shifted from 3469.62 to 3469.08 cm^{-1} , which had no significant difference. Moreover, the NH peak wavenumber of drug–LIPEX (control), drug–DPPG, and drug–ININ reduced by 1.46 cm^{-1} , 1.82 cm^{-1} , and 1.52 cm^{-1} , respectively, which were attributed to the intermolecular hydrogen bonds.

Molecular Modeling of Drug–Oil Interaction

The intermolecular interaction of drug and oils (squalane, ININ, and DPPG) were investigated using molecular modeling (28). Hydrogen bond was found between SPI and squalane as presented in Fig. 9a, but found in the complexes of both ININ–SPI and DPPG–SPI in Fig. 9b and c, and donor–acceptor distance was 3.156 Å and 2.837 Å. Moreover, the total energy for the formation of squalane–SPI, ININ–SPI, and DPPG–SPI were 183.49 , 90.31 , and 87.18 kcal/mol, respectively. The same trends were demonstrated in the key length, which indicated that SPI interacted with squalane through Van der Waals force and formed hydrogen bond with

Table I. Parameters of the emulsion containing different oils

Emulsion	C_{oil} (ug/ml)	C_{water} (ug/ml)	Average size (nm)	Apparent viscosity (mpa.s)
Squalene	3658.46 ± 58.43	52.67 ± 10.56	1140	1271 ± 52
LIPEX	3649.03 ± 46.71	56.30 ± 12.92	1042	1244 ± 64
ININ	3227.72 ± 48.54	43.74 ± 8.02	1595	1120 ± 45
DPPG	3389.41 ± 50.89	36.10 ± 9.24	1398	1211 ± 48

C_{oil} , the drug concentration in the oil layer, C_{water} , the drug concentration in the water layer

ININ and DPPG. The lower total energy of the mixing and smaller key length both indicated the stronger interaction strength (29).

In Vivo Tissue Distribution Study

As can be seen from Fig. 10, the rank order of drug content was listed as follows: skin > muscle > plasma. The drug retention amount was highest at 4 h in the skin, and relatively steady in the muscle. For the blood, the drug concentration could be detected in the first 2 h, indicating that a small amount of drug was absorbed into the blood through the skin. Moreover, concentration of drug in the tissues decreased rapidly when the emulsion was removed completely 8 h later.

Pharmacodynamics Study

Appearance of skin in photoaged rats were shown in the Fig. 11. It was found that the back skin of rats in the positive control group (b) had mild erythema; the skin color deepened with emergence of serious cracks and shrinkage than blank group (a). The negative group (c) had no obvious improvement. At last, wrinkle and erythema were improved in the emulsion group (d).

The content of hydroxyproline in photoaging skin was determined. In the blank group, the level of hydroxyproline was the highest ($30.67 \pm 2.47 \mu\text{g/g}$). When the rats were exposed to UV lamp, the content of hydroxyproline decreased significantly ($p < 0.05$). The hydroxyproline content was $14.75 \pm 1.84 \mu\text{g/g}$ and $15.55 \pm 2.03 \mu\text{g/g}$ in the positive and

negative group, respectively. It was proved that blank matrix had no therapeutic effect. Moreover, the hydroxyproline content was $23.99 \pm 2.21 \mu\text{g/g}$ in the emulsion group and increased significantly ($p < 0.05$). It was demonstrated that emulsion increased the content of collagen in the skin and played an important role in the recovery of photoaged skin.

The Safety Evaluation

Skin irritation results were presented in Fig. 12. The rats in the positive group were showing strong skin irritation, which proved that animal skin responded to stimuli. And the rats in the emulsion groups have no skin irritation reaction, which demonstrated that the emulsion was safe.

DISCUSSION

According to the results of anti-aging evaluation in the present study, the optimized SPI emulsion showed good pharmacodynamic effects due to high drug-skin retention. Thus, skin retention was a key parameter in the present study.

In the present study, it was indicated that drug-skin retention was determined by two factors: drug-skin miscibility and drug release amount from the emulsion. On the one hand, transdermal drug absorption behavior was mainly dependent on drug-skin miscibility. The fraction that SPI dissolved in skin was much higher than that in water according to the result of drug-skin miscibility study; thus, it was indicated that drug was mainly distributed in the skin, rather than crossed the skin into the blood. The results of

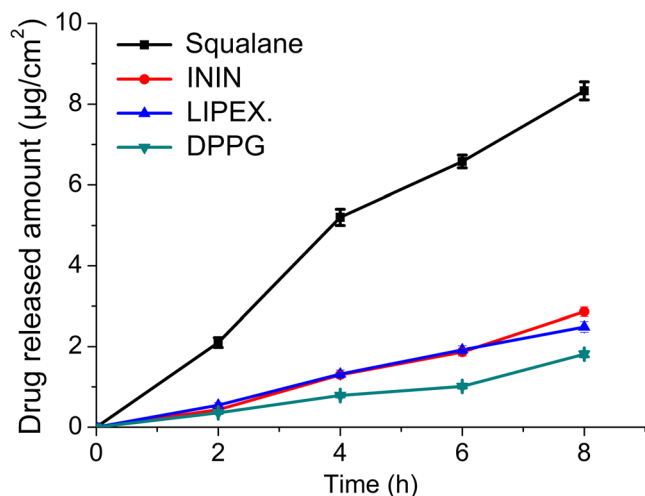


Fig. 6. The effect of oils on *in vitro* drug release ($n = 4$)

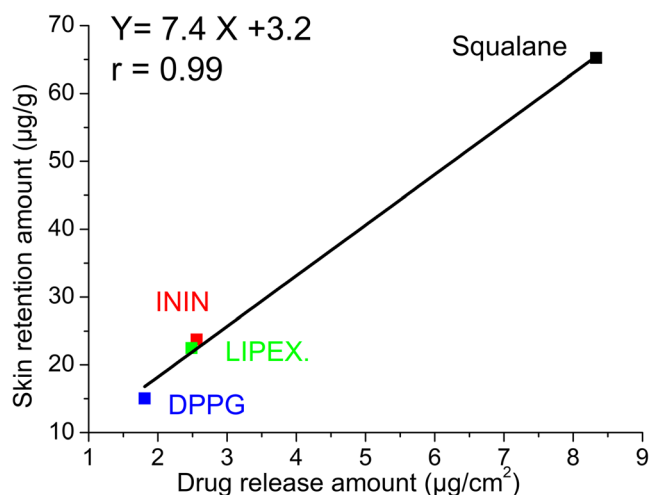


Fig. 7. The correlation analysis between drug release amount and skin retention amount

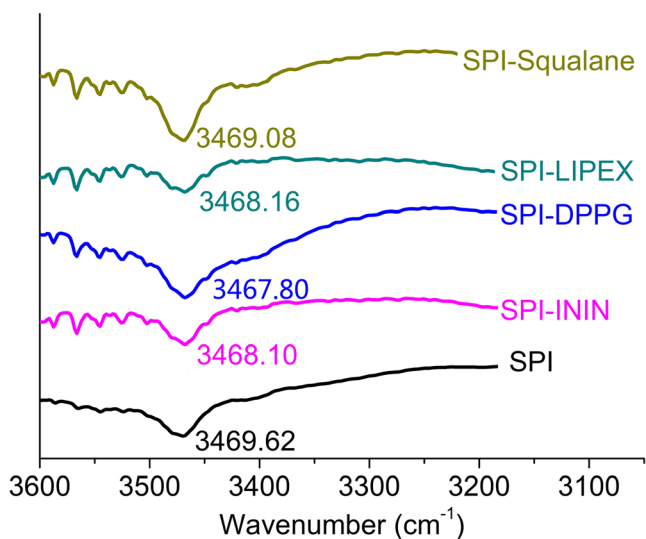


Fig. 8. IR spectra of SPI-oils system

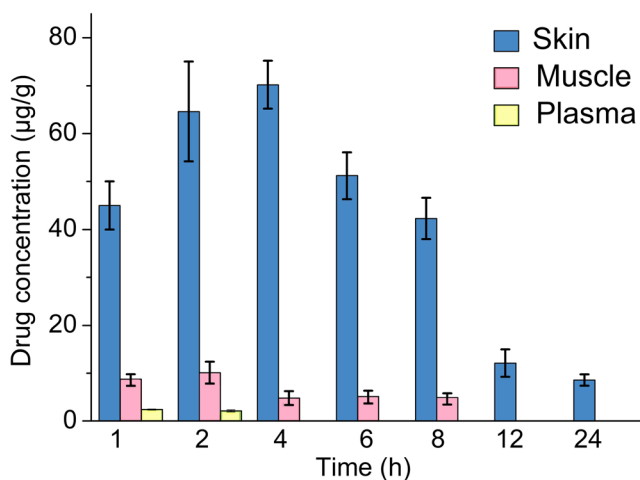


Fig. 10. The *in vivo* distribution of SPI in different tissues (*n* = 4)

molecular modeling demonstrated that the system of SPI-CerNS was more stable than SPI-water, indicating SPI had an excellent miscibility with CerNS and was mainly maintained

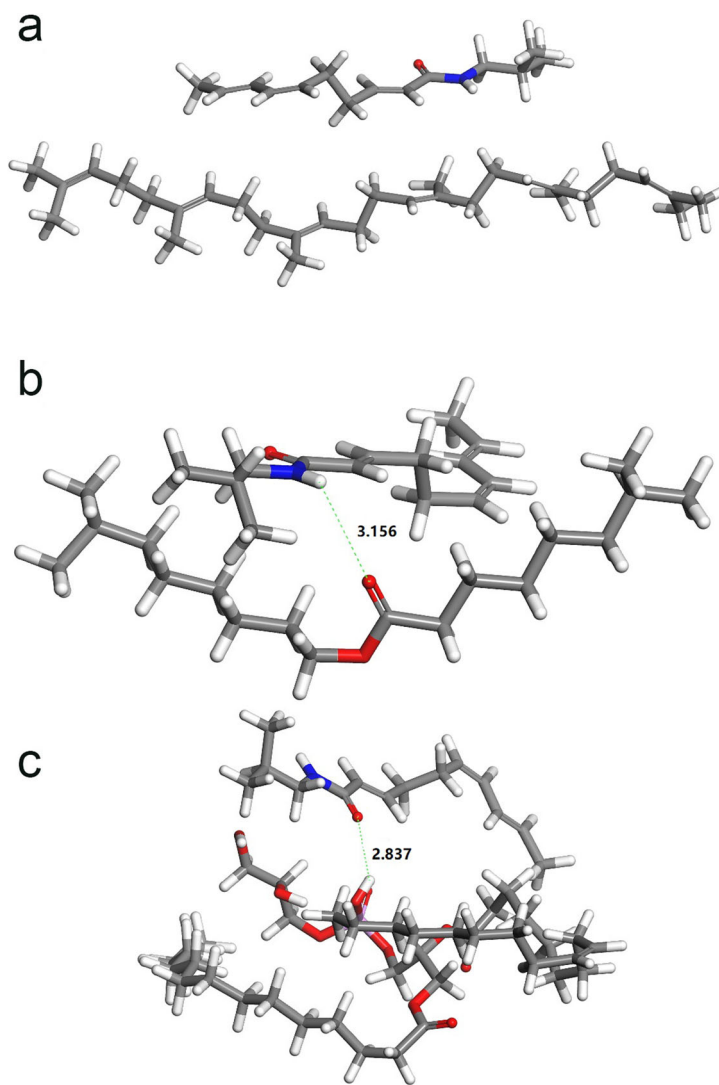


Fig. 9. Molecular modeling of SPI in three oils: a squalane; b ININ, and c DPPG

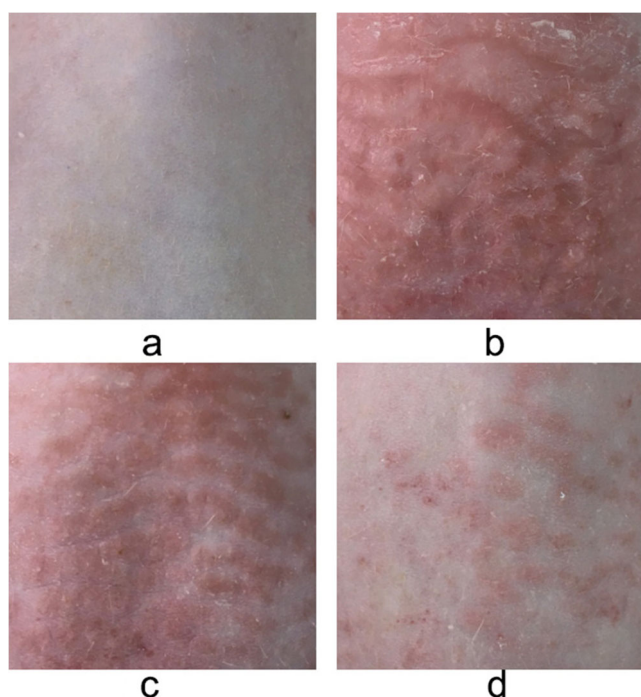


Fig. 11. The pictures of the appearance of skin in photoaged rats: **a** the blank group, **b** the positive control group, **c** the negative group, and **d** the emulsion group

in the stratum corneum. Thus, drug–skin permeation amount maintained a low level in all preparations, and the released drug was able to store in the skin lipid layer.

Drug release was the rate limiting step for SPI emulsion. A revised equation was applied to skin topical action according to the equation proposed by Guy and Hadgraft (30):

$$F = \frac{R}{M} \quad (4)$$

where M was the cumulative amount of drug released and R was skin retention amount. If $F=1$ or close to 1, it was implied that the drug was entirely controlled by the drug release from emulsion; when $F < 1$, the skin was also responsible for the control process. In the present study, the rate limiting step of SPI transdermal drug delivery was determined as follows: $F_{R/M}=0.81$. Thus, drug release was the rate limiting step in the transdermal drug delivery process. Besides, drug distribution study (Table I) demonstrated that most drugs existed in the oil phase. Thus, it was concluded that oil phase controlled the drug release process thus demonstrated a significant effect on the drug delivery process of SPI in emulsion.

Therefore, the present study was focused on the effect of oil on the release behavior at the molecular level. As shown in Table I, the emulsions prepared using four oils were controlled and similar droplet size and apparent viscosity were obtained. Thus, molecular interaction became the prominent factor that affected the drug release process. Furthermore, as depicted in Fig. 8, significant wavenumber variations were observed in the FT-IR spectra after the mixture of drug and oil: (1) there was no significant NH peak

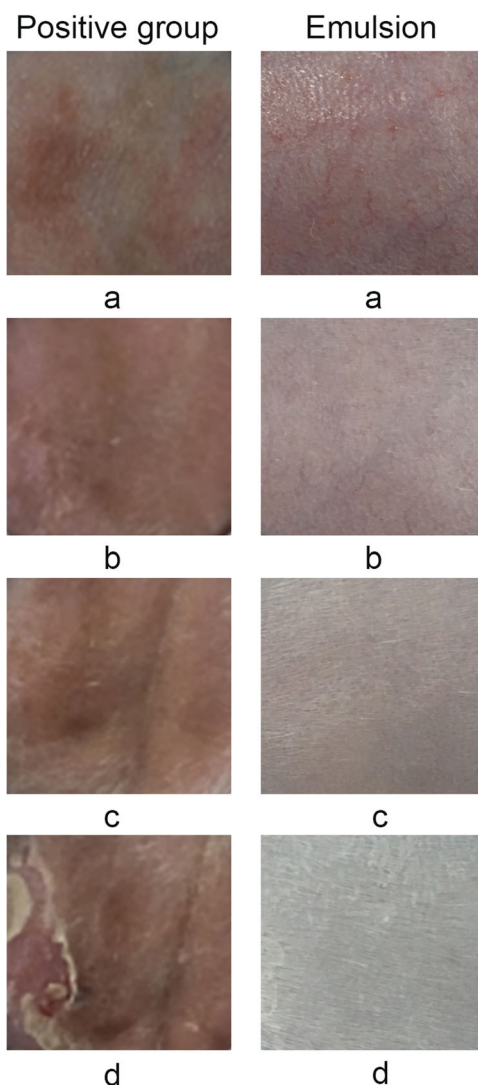


Fig. 12. The images depicting the skin irritation area recorded after 1 (**a**), 24 (**b**), 48 (**c**), and 72 h (**d**)

(SPI) shift when squalene was added. An explanation for the shift was that squalene was the structure of alkenes and was not a hydrogen-bond donor or acceptor. Thus, there was no hydrogen bond, and Van der Waals force might exist between the drug and squalene, which was much weaker than the hydrogen bond. (2) Blue shift indicated that the hydrogen bonds were formed in the mixtures of drug–LIPEX (control), drug–DPPG, and drug–ININ. And the biggest blue shift value and the strongest interaction strength between drug and DPPG was obtained, which contained several hydrogen-bond acceptors and hydrogen-bond donors. LIPEX and ININ both contained an ester group, which was only a medium hydrogen-bond acceptor. The results of drug–oil interaction were consistent with the drug release results. Moreover, this was further substantiated by the results of molecular modeling. The molecular modeling results (Fig. 9) demonstrated the presence of Van der Waals force between SPI and squalane. In addition, Van der Waals was significantly weaker than the hydrogen bond formed between ININ and DPPG, which proved that weaker interaction strength caused the higher drug release behavior (31). Moreover, bond length and total

energy of the complex showed a significant difference ($p < 0.05$). The results mentioned above showed that the drug–oil interaction strength influenced the release behavior. The mechanism investigation of the drug release provided reference for the research of formulation optimization.

Tissue distribution study showed that concentration of SPI in the skin was significantly higher than muscles and plasma ($p < 0.05$), which indicated that SPI was a local action and may avoid systemic side effects. Afterwards, photoaging rats were chosen as the model in the pharmacodynamic evaluation, and their effectiveness was investigated by measuring the content of hydroxyproline, which provided a basis for the wide application of emulsion. Hydroxyproline accounted for 13.14% of collagen and was extremely small in other proteins (32). As a result, the content of hydroxyproline could be converted into collagen to reflect the degree of skin aging. The results of pharmacodynamics study (Fig. 11) demonstrated that the skin of photoaged rats administrated with optimized emulsion was much better than the blank group and the amount of collagen increased significantly, which fully proved that emulsion was effective and played a role in the repair of photoaging skin. Moreover, skin irritation experiments both proved that the prepared emulsion was safe and nonirritating. Nowadays, the design of emulsion formulation was in blindness under the circumstance of lack of basic theory. Especially for local efficacy, the issues about the release and skin retention properties of the drug need to be solved urgently. To figure out such issues, the study investigated the drug–skin miscibility and effect of interaction strength between drug and oils on drug release, which provided scientific method and primary theory for the design of emulsion.

CONCLUSION

In the present study, a safe and effective emulsion containing SPI was developed successfully and evaluated systematically. And effects of oil and drug physicochemical properties on drug release and skin retention at molecular level were investigated. The results demonstrated that oil acted as a drug reservoir in the emulsion and oil–drug interaction played a dominant role in the drug-controlled release process. And released drug was stored in the skin due to good drug–skin miscibility, which obtained the maximum skin retention and excellent anti-aging efficacy. Thus, this study provided a good understanding of drug–excipient interaction and drug physicochemical properties on drug release and skin retention of emulsion at a molecular level and provided references for the formulation design of emulsion.

FUNDING INFORMATION

This work was supported by the National Natural Science Foundation of China (81803468).

COMPLIANCE WITH ETHICAL STANDARDS

All the procedures were performed in accordance with the NIH Guidelines for the Care and Use of Laboratory Animals and were approved by the Animal Ethics Committee of Shenyang Pharmaceutical University. The ethical review number was SYPU-IACUC-C2018-12-5-207.

Conflict of Interest The authors declare that they have no conflicts of interest.

REFERENCES

- Prachayasittukul V, Prachayasittukul S, Ruchiwarat S, Prachayasittukul V. High therapeutic potential of *Spilanthes acmella*: a review. *EXCLI J*. 2013;12:291–312.
- Veryser L, Wynendaele E, Taevernier L, Verbeke F, Joshi T, Tatke P. N-alkylamides: from plant to brain. *Func Foods Health Dis*. 2014;4:264–75.
- Dandin VS, Naik PM, Murthy HN, Park SY, Lee EJ, Paek KY. Rapid regeneration and analysis of genetic fidelity and scopoletin contents of micropropagated plants of *Spilanthes oleracea* L. *J Hort Sci Biotechnol*. 2014;89:79–85.
- Kim SK. Marine emulsion. *J Cosmet Dermatol*. 2014;13:56–67.
- Boonen J, Halet E, Burvenich C, Spiegeleer BD. Transdermal behaviour of the N-alkylamide spilanthol (affinin) from *Spilanthes acmella* (Compositae) extracts. *J Ethnopharmacol*. 2010;127:77–84.
- Spiegeleer B, Boonen J, Malysheva S, Mavungu J, Saeger S, Roche N, et al. Skin penetration enhancing properties of the plant N-alkylamide spilanthol. *J Ethnopharmacol*. 2013;148:117–25.
- Boonen J, Baert B, Burvenich C, Blondeel P, De Saeger S, De Spiegeleer B. LC-MS profiling of N-alkylamides in *Spilanthes acmella* extract and the transmucosal behaviour of its main bioactive spilanthol. *J Pharmaceut Biomed*. 2010;53:243–9.
- Demarne F, Passaro G. Use of an *Acmella oleracea* extract for the botulinum toxin-like effect thereof in an emulsion cosmetic composition. US Patent. No. 7,531,193 B2, 2009.
- Sherif S, Bendas ER, Badawy S. The clinical efficacy of cosmeceutical application of liquid crystalline nanostructured dispersions of alpha lipoic acid as emulsion. *Eur J Pharm Biopharm*. 2014;86:251–9.
- Jaworska M, Sikora E, Zielina M, Ogonowski J. Studies on the formation of O/W nano-emulsions, by low-energy emulsification method, suitable for cosmeceutical applications. *Acta Biochim Pol*. 2013;60:779–82.
- Storsberg J, Laughton MW, Geyer M, Vollrath MK, Schmidt C. IL16 – improving the bioavailability of pharmacologically active substances in pharmaceutical and cosmetic formulations. *Asian J Pharm Sci*. 2016;11:33–4.
- Salmela L, Washington C. A continuous flow method for estimation of drug release rates from emulsion formulations. *Int J Pharm*. 2014;472:276–81.
- Paukkonen H, Ukkonen A, Szilvay G, Yliperttula M, Laaksonen T. Hydrophobin-nanofibrillated cellulose stabilized emulsions for encapsulation and release of BCS class II drugs. *Eur J Pharm Sci*. 2017;100:238–48.
- Ajazuddin, Alexander A, Khichariya A, Gupta S, Patel R, Giri T, et al. Recent expansions in an emergent novel drug delivery technology: Emulgel. *J Control Release*. 2013;171:122–32.
- Alexander A, Dwivedi S, Ajazuddin, Giri TK, Saraf S, Saraf S. Approaches for breaking the barriers of drug permeation through transdermal drug delivery. *J Control Release*. 2012;164:26–40.
- Narang AS, Desai D, Badawy S. Impact of excipient interactions on solid dosage form stability. *Pharm Res*. 2012;29:2660–83.
- Thiry J, Broze G, Pestieau A, Tatton AS, Baumans F, Dambon C, et al. Investigation of a suitable in vitro dissolution test for itraconazole-based solid dispersions. *Eur J Pharm Sci*. 2016;85:94–105.
- Xi HL, Cun DM, Wang ZY, Shang L, Fang L. Effect of the stability of hydrogen-bonded ion pairs with organic amines on transdermal penetration of teriflunomide. *Int J Pharm*. 2012;436:857–61.

19. Wang ML, Xi HL, Cun DM, Chen Y, Xu YN, Fang L. l-Carvyl esters as penetration enhancers for the transdermal delivery of 5-fluorouracil. *AAPS PharmSciTech*. 2013;14:669–74.
 20. Fedors R. A method for estimating both the solubility parameters and the molar volumes of liquids. *Polym Eng Sci*. 1974;14:147–54.
 21. Fedors R. Osmotic effects in water absorption by polymers. *Polymer*. 1980;21:207–12.
 22. Adeleke O, Monama N, Tsai P-C, Sithole H, Michniak-Kohn B. Combined atomistic molecular calculations and experimental investigations for the architecture, screening, optimization, and characterization of pyrazinamide containing oral film formulations for tuberculosis management. *Mol Pharm*. 2016;13:456–71.
 23. Dai X, Shi X, Yin Q, Ding H, Qiao Y. Multiscale study on the interaction mechanism between ginsenoside biosurfactant and saikosaponina. *J Colloid Interface Sci*. 2013;396:165–72.
 24. Nan L, Liu C, Li Q, Wan X, Guo J, Quan P, et al. Investigation of the enhancement effect of the natural transdermal permeation enhancers from *Ledum palustre* L. var. *angustum* N. Busch: mechanistic insight based on interaction among drug, enhancers and skin. *Eur J Pharm Sci*. 2018;124:105–13.
 25. Choi H, Park E, Park Y, Suh H. Spent coffee ground extract suppresses ultraviolet B-induced photoaging in hairless mice. *J Photochem Photobiol B*. 2015;153:164–72.
 26. Haratake A, Watase D, Setoguchi S, Nagata-Akaho N, Matsunaga K, Takata J. Effect of orally ingested diosgenin into diet on skin collagen content in a low collagen skin mouse model and its mechanism of action. *Life Sci*. 2017;174:77–82.
 27. Li C, Wang J, Le Y, Chen J. Studies of bicalutamide–excipients interaction by combination of molecular docking and molecular dynamics simulation. *Mol Pharm*. 2013;10:2362–9.
 28. Song W, Quan P, Li S, Liu C, Lv S, Zhao Y, et al. Probing the role of chemical enhancers in facilitating drug release from patches: mechanistic insights based on FT-IR spectroscopy. Molecular modeling and thermal analysis. *J Control Release*. 2016;227:13–2.
 29. Nilsson L, Widdifield C, Pettersen A, Svensk A, Lindkvist M, Aldred P, et al. Elucidating an amorphous form stabilization mechanism for tenapanor hydrochloride: crystal structure analysis using X-ray diffraction, NMR crystallography, and molecular modeling. *Mol Pharm*. 2018;15:1476–87.
 30. Guy R, Hadgraft J. Rate control in transdermal drug delivery? *Int J Pharm*. 1992;82:1–6.
 31. Liu C, Quan P, Fang L. Effect of drug physicochemical properties on drug release and their relationship with drug skin permeation behaviors in hydroxyl pressure sensitive adhesive. *Eur J Pharm Sci*. 2016;93:437–46.
 32. Hall D, Reed R. Hydroxyproline and thermal stability of collagen. *Nat*. 1957;180:24.
- Publisher's Note** Springer Nature remains neutral with regard to jurisdictional claims in published maps and institutional affiliations.